Available online at www.sciencedirect.com
SCIENCE DIRECT®
Geochimica et Cosmochimica Acta 70 (2006) 2643–2657
Geochimica
www.elsevier.com/locate/gca

Large thallium isotopic variations in iron meteorites and evidence for lead-205 in the early solar system

Sune G. Nielsen [a,b,*], Mark Rehkämper [a,c], Alex N. Halliday [a,d]

[a] Department of Earth Sciences, ETH Zurich, Sonneggstrasse 5, 8092 Zurich, Switzerland
[b] GEMOC, Department of Earth and Planetary Sciences, Macquarie University, NSW 2109, Australia
[c] Department of Earth Science and Engineering, Imperial College, London SW7 2AZ, UK
[d] Department of Earth Sciences, University of Oxford, Parks Road, Oxford OX1 3PR, UK

Received 1 September 2005; accepted in revised form 22 February 2006

Abstract

Lead-205 decays to ^{205}Tl with a half-life of 15 Myr and should have been present in the early solar system according to astrophysical models. However, despite numerous attempts, Tl isotopic measurements of meteorites have been unable to demonstrate convincingly its former presence. Here, we report large (~5‰) variations in Tl isotope composition in metal and troilite fragments from a range of iron meteorites that were determined at high precision using multiple collector inductively coupled plasma mass spectrometry. The Tl isotopic compositions of seven metal samples of the IAB iron meteorites Toluca and Canyon Diablo define a correlation with ^{204}Pb/^{203}Tl. When interpreted as an isochron, this corresponds to an initial ^{205}Pb/^{204}Pb ratio of $(7.4 \pm 1.0) \times 10^{-5}$. Alternative explanations for the correlation, such as mixing of variably mass-fractionated meteorite components or terrestrial contamination are harder to reconcile with independent constraints. However, troilite nodules from Toluca and Canyon Diablo contain Tl that is significantly less radiogenic than co-existing metal with isotope compositions that are variable and decoupled from ^{204}Pb/^{203}Tl. These effects are similar to those recently reported by others for Fe and Ni isotopes in iron meteorite sulfides and appear to be the result of kinetic stable isotope fractionation during diffusion. Though it cannot conclusively be shown that the metal fragments are unaffected by the secondary processes that disturbed the troilites, mass balance modeling indicates that the alteration of the troilites is unlikely to have significantly affected the Tl isotope compositions of the co-existing metals. It is therefore reasonable to conclude that the IAB metal isochron is a product of the in situ decay of ^{205}Pb. If the I–Xe ages of IAB silicate inclusions record the same event as the ^{205}Pb–^{205}Tl chronometer then crystallization of the IAB metal was probably completed between 10 and 20 Myr after the condensation of the first solids. This implies an initial solar system ^{205}Pb/^{204}Pb of $(1.0–2.1) \times 10^{-4}$, which is in excellent agreement with recently published astrophysical predictions. Similar calculations yield an initial solar system Tl isotope composition of $\varepsilon^{205}\text{Tl} = -2.8 \pm 1.7$. The Tl isotopic composition and concentration of the silicate Earth depends critically on the timing and mechanism of core formation and Earth's volatile element depletion history. Modeling of the Earth's accretion and core formation using the calculated initial solar system Tl isotope composition and ^{205}Pb/^{204}Pb, however, does not yield reasonable results for the silicate Earth unless either the Earth lost Tl and Pb late in its accretion history or the core contains much higher concentrations of Pb and Tl than are found in iron meteorites.

1. Introduction

Investigations of extinct radionuclides present in the early solar system can provide information on the presolar production sites of elements and the timescales of early solar system processes. The nuclide ^{205}Pb, which decays to ^{205}Tl with a half-life of 15.1 ± 0.4 Myr (Pengra et al., 1978), is of particular significance in this regard. For astrophysicists, ^{205}Pb offers a unique opportunity to study nucleosynthetic mechanisms because it is the only short-lived radionuclide that is produced solely by the s-process (Wasserburg et al., 1994), whereby heavier elements are

* Corresponding author.
E-mail address: snielsen@els.mq.edu.au (S.G. Nielsen).

0016-7037/$ - see front matter © 2006 Elsevier Inc. All rights reserved.
doi:10.1016/j.gca.2006.02.012

formed by slow neutron capture in the interior of stars. Both Pb and Tl are somewhat chalcophile and/or siderophile and the elements are volatile with half mass condensation temperatures of 727 and 532 K, respectively (Lodders, 2003). Thus, the Tl and ^{204}Pb concentrations of the bulk silicate Earth (BSE) are a function of the volatile element depletion history of the Earth as well as their respective partitioning into the core. The ^{205}Pb–^{205}Tl decay system may therefore also prove to be useful for dating volatile loss and planetary differentiation.

A number of previous studies have attempted to find evidence of formerly live ^{205}Pb in meteorites and establish the initial solar system abundance of this isotope (Anders and Stevens, 1960; Chen and Wasserburg, 1994b; Huey and Kohman, 1972). All of these investigations were unsuccessful, mainly because they utilized thermal ionization mass spectrometry, which is unable to provide sufficiently precise Tl isotope data. Only an upper limit for the initial solar system ^{205}Pb/^{204}Pb ratio of less than 9×10^{-5} is, therefore, currently available (Anders and Stevens, 1960; Huey and Kohman, 1972; Chen and Wasserburg, 1994b) but this figure may be too low if the high Pb/Tl ratios that were reported for some samples are due to contamination with terrestrial Pb. More recent analyses (Chen and Wasserburg, 1987) revealed a ''hint'' of excess ^{205}Tl for an iron meteorite, but this effect was barely resolved. Moreover, a sulfide analyzed by Chen and Wasserburg (1987) was reported to have a very low (unradiogenic) ^{205}Tl/^{203}Tl isotope ratio that was difficult to reconcile with the other results.

In the present study, we have utilized the technique of multiple collector inductively coupled plasma mass spectrometry (MC-ICPMS) because this enables us to determine the isotopic composition of less than 1 ng of Tl, to a precision over an order of magnitude better than previously possible (Rehkämper and Halliday, 1999; Nielsen et al., 2004b). The low initial ^{205}Pb/^{204}Pb ratio estimated by Huey and Kohman (1972) implies that only samples with high Pb/Tl should exhibit resolvable Tl isotope anomalies, even with our improved analytical techniques. We have therefore, concentrated our efforts on the analyses of iron meteorites because these are known from Pd–Ag and Hf–W isotope studies to have formed early (Chen and Wasserburg, 1996; Lee and Halliday, 1996; Horan et al., 1998) and because they display highly fractionated Pb/Tl ratios (Chen and Wasserburg, 1994a).

We have analyzed both metal fragments and troilite inclusions from iron meteorites of groups IAB, IIAB, and IIIAB. These samples were selected so as to obtain as large a spread in Pb/Tl ratio as possible and to enhance the probability of observing Tl isotope variation from the decay of ^{205}Pb. Moreover, we have analyzed six separate metal fragments of the IAB iron Toluca. By analogy with studies of Ag isotopes in iron meteorites (Chen and Wasserburg, 1990), it was anticipated that these samples could yield an internal Pb–Tl isochron that would provide improved constraints on the initial abundance of ^{205}Pb in the early solar system.

2. Analytical techniques

2.1. Sample preparation

The iron meteorite samples, about 7–40 g of metal or 1–3 g of sulfide, were cut and alteration surfaces removed using a diamond-coated saw blade. The samples were then cleaned by repeated leaching with aqua regia followed by washing with 18 MΩ-grade water, until only a shiny central piece remained. This material, equivalent to about 70–95% of the original mass was weighed, dissolved in aqua regia, dried down, and taken up in an appropriate volume of 1 M HCl and bromine water (Rehkämper and Halliday, 1999). An aliquot equivalent to about 5% of the total sample was then removed from the beakers for the determination of the Pb and Tl concentrations and Pb/Tl ratios. The remaining solution (~95%) was used for the Tl isotopic measurements.

2.2. Thallium separation and procedural blank

A two-stage column chromatographic technique with anion-exchange resin was used to isolate Tl from the sample matrix (Nielsen et al., 2004b). Due to the extreme partitioning of Tl^{3+} onto the AG1 X 8 resin used ($D > 10^5$), it is possible to process large amounts of sample without any loss of Tl. Consequently, yields throughout this study were $100 \pm 10\%$, where the uncertainty is similar to the precision of the technique that was used for the yield determination (Rehkämper et al., 2002). The only samples with lower yields (of ~75%) are the metal fragment and troilite from Grant and the Mundrabilla troilite. In these cases, the yield estimates may be too low, however, because the small amounts of Tl available led to inaccuracies in the yield measurements. The total procedural blank was less than 3 pg Tl, if 500 ml of acid (aqua regia and 1 M HCl) was used for sample digestion. Such a volume suffices to dissolve samples of about 20 g. Given that all isotopic analyses utilized >100 pg Tl, the contribution of the blank to the total Tl content of a sample is less than 3%, which is insignificant.

2.3. Determination of Tl isotope compositions

The Tl isotope compositions were determined by MC-ICPMS at the ETH Zurich using previously described techniques that utilize both external normalization to NIST SRM 981 Pb and standard-sample bracketing for mass bias correction (Rehkämper and Halliday, 1999; Nielsen et al., 2004b). The isotopic results are reported as the deviation of a sample from the NIST SRM 997 Tl isotopic standard in parts per 10,000:

$$\varepsilon^{205}\mathrm{Tl} = 10,000 \times \left(^{205}\mathrm{Tl}/^{203}\mathrm{Tl}_{\mathrm{sample}} - {}^{205}\mathrm{Tl}/^{203}\mathrm{Tl}_{\mathrm{SRM\ 997}}\right) / \left(^{205}\mathrm{Tl}/^{203}\mathrm{Tl}_{\mathrm{SRM\ 997}}\right). \quad (1)$$

Table 1
Long-term reproducibility of Tl isotope data obtained at low ion beam intensities for the Fe–Mn nodule NOD-A-1

ε^{205}Tl	Total Tl ion beam ($\times 10^{-11}$ A)	Deviation from $\varepsilon^{205}Tl = 10.7$[a]
9.7	0.20	1.0
12.7	0.20	2.0
10.7	0.26	0.0
11.4	0.27	0.7
11.3	0.32	0.6
10.2	0.33	0.5
9.3	0.34	1.4
10.1	0.35	0.6
10.4	0.39	0.3
11.4	0.39	0.7
11.3	0.48	0.6
11.2	0.50	0.5
11.0	0.52	0.3
11.2	0.54	0.5
10.7	0.83	0.0
12.0	0.84	1.3
10.3	0.85	0.4
11.5	0.86	0.8
11.5	0.94	0.8
11.0	0.95	0.3

[a] Reference value from Nielsen et al. (2004b).

The uncertainties of the isotope data reflect the 2σ external reproducibility obtained for multiple analyses of the Fe–Mn nodule NOD-A-1 (Nielsen et al., 2004b), as performed at ion beam intensities equivalent to those encountered in the iron meteorite analyses (Table 1). This sample (which is a USGS reference material) had previously been analyzed repeatedly over a period of several months at total Tl ion beam intensities $>10 \times 10^{-11}$ A, and these measurements yielded a reference value and long-term reproducibility of $\varepsilon^{205}Tl = 10.7 \pm 0.5$ (Nielsen et al., 2004b). Based on the data of Table 1, the following uncertainties are applied to the iron meteorite analyses: ± 2 ε^{205}Tl for total Tl ion beams of $0.2–0.5 \times 10^{-11}$ A, ± 1.5 ε^{205}Tl for $0.5–1.0 \times 10^{-11}$ A, and ± 1 ε^{205}Tl for total Tl ion beams of $>1.0 \times 10^{-11}$ A. The isotope composition measurements of the metal samples from Murphy (USNM 557), Mount Edith (USNM 528) and Grant were performed at Tl ion beam intensities of 0.14, 0.18, and 0.07×10^{-11} A, respectively, and these samples are assigned an uncertainty of ± 3 ε^{205}Tl.

2.3.1. Isobaric interferences

No direct isobaric interferences exist on ^{203}Tl or ^{205}Tl. In a previous study we conducted a thorough investigation of possible molecular interferences arising from different sample matrices (Nielsen et al., 2004b). It was concluded that the column chemistry leaves no appreciable amounts of elements with atomic weights >100 amu in the purified Tl fractions. For this study, the Tl sample solutions of iron meteorites were scanned over the mass range 120–202 amu in order to identify whether some elements specific to iron meteorites were present. The only elements detected were Pt, Ir, and Re, which were all present in minor amounts, such that the total ion beam intensities yielded ratios of Re/Tl < 0.001, Pt/Tl < 0.2, and Ir/Tl < 0.005. Realistically, only di-atomic molecules with O, N, or Ar could potentially create significant spectral interferences because the production rates of polyatomic molecules are typically very low (Nielsen et al., 2004b). Platinum oxides or nitrides can only create interferences on Pb, which can be detected by internally normalizing ^{207}Pb/^{206}Pb to ^{208}Pb/^{206}Pb. Such effects have not been observed for any samples analyzed in this study. In addition, we tested for potential spectral interferences from Re and Ir, by adding these elements to mixed Pb–Tl standard solutions, to achieve Re/Tl and Ir/Tl ratios higher (with total ion beam ratios of Re/Tl > 0.02, Ir/Tl > 3) than those observed for the iron meteorite samples. None of these tests generated any isotopic offsets from spectral interferences and other inconsistencies were not observed.

2.3.2. Matrix doping tests

In a previous investigation, we evaluated whether the Tl isotope analyses of seawater with very high matrix/Tl ratios suffered from matrix effects that generate inaccurate results. We were able to rule out such a bias, based on a number of "matrix tests" (Nielsen et al., 2004b). Iron meteorites also have very high matrix/Tl ratios and we have therefore performed additional experiments that specifically test for the matrix effects of iron meteorites. These tests utilized the Tl-free matrix of a sample (obtained from the anion-exchange separation), which was doped with an amount of the NIST SRM 997 Tl isotope standard (which defines $\varepsilon^{205}Tl = 0$), to obtain a Tl content similar to that of the original iron meteorite. These synthetic samples were then reprocessed and analyzed in the same manner as the meteorites. Four separate experiments were completed, three of which used the matrix of the Toluca metal samples Ir-30n-1, Ir-30n-2, and Toluca C doped with 0.5, 0.2, and 1 ng of SRM NIST 997 Tl, respectively (Table 2). A fourth test utilized 100 mg of pure elemental sulfur that was doped with 15 ng of SRM NIST 997 Tl. The sulfur–Tl mixture was then dissolved in aqua regia, dried down, and thereafter processed as a normal sample. As is evident from Table 2, all analyses yielded results that are within error of the true result of $\varepsilon^{205}Tl = 0$, which demonstrates the absence of any significant matrix effects.

2.3.3. Evaluation of matrix effects by monitoring the mass bias of samples and standards

The Tl isotope analyses utilize external normalization to Pb for the correction of instrumental mass discrimination. This procedure assumes that the relative mass bias of Pb and Tl is identical for samples and bracketing standards (Nielsen et al., 2004b). Inaccuracies caused by matrix effects in MC-ICPMS measurements are often accompanied by significant drift in mass bias during sample runs or large differences in absolute mass bias between samples and standards. No significant drift was observed in the mass bias of any sample runs during the course of this

Table 2
Mass bias offset of samples compared to bracketing standards and Tl isotope data obtained for individual sample analyses and matrix tests

Sample	$\Delta\beta^{208/206}$	ε^{205}Tl	$\Delta\beta^{208/206}$ repeat	ε^{205}Tl repeat
Metals				
Canyon Diablo	−0.024	−1.8		
Toluca AB	0.024	14.2		
Toluca C	0.018	16.7		
Toluca Ir-30m	0.057	11.9		
Toluca Ir-30n-1	0.003	−1.3	−0.015	−1.5
Toluca Ir-30n-2	0.013	−2.4	−0.054	−3.0
Toluca USNM 75	0.007	23.3		
Murphy USNM 557	−0.029	0.9		
Navajo USNM 5601	−0.003	−1.6		
Mount Edith USNM 528	0.024	16.1		
Grant	0.043	18.9		
Mundrabilla A	−0.030	29.7	0.018	30.0
Mundrabilla B	−0.012	28.8	0.029	29.5
Sulfides				
Canyon Diablo USNM 676 A	0.006	−18.8	−0.057	−19.2
Canyon Diablo USNM 676 B	0.022	−6.4		
Toluca USNM 75	0.016	−12.6	0.012	−13.2
Toluca Ir-30m	−0.039	11.2	−0.017	10.4
Toluca Ir-30a[a]	−0.031	−6.0		
Grant	0.009	−3.4		
Mundrabilla	0.006	24.2		
Matrix tests				
Ir-30n-1 + 0.5 ng Tl	−0.038	0.1		
Ir-30n-2 + 0.2 ng Tl	−0.046	−0.4		
100 mg sulfur + 15 ng Tl	0.015	0.3		
Toluca C + 1 ng Tl	−0.043	0.6		

$\Delta\beta^{208/206}$ denotes the difference between the average $^{208}Pb/^{206}Pb$ β value of the standards analyzed before and after a sample and the $^{208}Pb/^{206}Pb$ β value of the sample measurement. All individual sample analyses have a minimum of four bracketing standards (two before and two after).

[a] Sample Toluca Ir-30a consisted of metal, with a large sulfide inclusion trapped in the center.

study. Additionally, the external normalization technique, which is applied in this study, allows monitoring of the Pb mass bias for both standards and samples. A comparison of the β values (mass bias coefficients) obtained for samples and the bracketing standards therefore provides a good indication of potential matrix effects. In Table 2, the difference between the β value for sample runs and the bracketing standards are listed as $\Delta\beta^{208/206}$, which denotes the difference of the $^{208}Pb/^{206}Pb$ β value for samples and their bracketing standards. Several observations are significant with regard to Table 2. First, it can be seen that the differences in mass bias are small between samples and bracketing standards. Second, there is no systematic offset in mass bias between samples and standards; that is, the samples do not always display higher or lower mass bias coefficients than the standards. Third, the mass bias offsets of the matrix tests ($\Delta\beta^{208/206}$ up to −0.046), which do not display any analytical artifacts, are similar to the offsets for all other samples. Hence, mass bias offsets of this magnitude recorded for the samples should not induce analytical artifacts either. Fourth, repeat analyses of sample solutions (only performed for samples with high Tl concentrations as the entire sample is consumed in one analysis for Tl-poor samples) all reproduce to well within the error of ±1 ε^{205}Tl. This is the case even when the duplicate analyses exhibit a difference in $\Delta\beta^{208/206}$ of up to 0.067 (Ir-30n-2), which is the largest mass bias offset recorded in this study.

2.4. Determination of Pb and Tl concentrations and $^{204}Pb/^{203}Tl$ ratios

All concentration measurements utilized the isotope dilution technique. To this end, the minor (5%) sample solution aliquots were spiked with enriched tracer solutions of ^{203}Tl and ^{208}Pb, dried down, and re-dissolved in 1 M HBr. Following this, Pb and Tl were separated from the sample matrix by anion-exchange chromatography using techniques modified from published procedures (Rehkämper and Halliday, 1999; Nielsen et al., 2004b). Some samples required two passes through the ion-exchange chemistry to obtain sufficiently pure Tl fractions, as in some instances significant residual Pb was present after the first pass. The separated fractions of Pb and Tl were then analyzed by MC-ICPMS, using added Pt for the external normalization of mass discrimination (Nielsen et al., 2004b).

Despite rigorous leaching, many of the analyzed samples showed evidence of contamination by terrestrial Pb, a problem that was previously encountered in other iron meteorite studies (Göpel et al., 1985; Chen and Wasserburg, 1994a). Typically, only a small fraction of this contamination could be attributed to the Pb blank of the dissolution and chemical separation procedure, even though this is relatively high at about 200–400 pg, owing to the large volumes of reagents used for sample preparation. Due to the high purity of the ^{208}Pb spike (>99.95% ^{208}Pb) we were, however, able to obtain sufficiently accurate primordial ^{204}Pb contents by correcting for this contamination. The fraction of terrestrial Pb present in any sample was determined by calculating the intersection of (1) the line that connects the measured Pb isotope compositions of the (contaminated and spiked) sample and the ^{208}Pb spike with (2) a mixing line that extends from the Pb isotope composition of the original meteoritic Pb to the isotope composition of the (assumed) terrestrial contaminant. These calculations were carried out in $^{208}Pb/^{206}Pb$ versus $^{207}Pb/^{206}Pb$ isotope space. Following Göpel et al. (1985), the original (uncontaminated) samples were assumed to have primordial Pb isotope compositions, whereas the terrestrial contaminant was defined by $^{207}Pb/^{204}Pb = 0.0898 \times {}^{206}Pb/^{204}Pb + 13.92$ and $^{208}Pb/^{204}Pb = 0.697 \times {}^{206}Pb/^{204}Pb + 25.3$, for $^{206}Pb/^{204}Pb$ values of between 17.65 and 18. Two "extreme" values for the Pb concentration and isotope composition of each sample were thus obtained by inserting values of 17.65 and 18 for $^{206}Pb/^{204}Pb$ into the contaminant equations. An additional calculation, which assigned the Pb isotope composition of the laboratory blank ($^{206}Pb/^{204}Pb = 17.726$, $^{207}Pb/^{204}Pb = 15.612$, and $^{208}Pb/^{204}Pb = 37.64$) to the contaminant, yielded a third set of results. The three datasets that were

produced in this way allowed a reliable estimate of the maximum and minimum primordial Pb contents of the samples, which served to provide a best estimate of the primordial ^{204}Pb concentrations and their respective uncertainty.

The Pb isotope data reported for each sample (Table 3) are calculated from the measured ^{207}Pb/^{206}Pb and ^{208}Pb/^{206}Pb isotope ratios of the isotope dilution runs by correcting for the Pb contributed by the ^{208}Pb spike. The errors reported for the Pb isotope data only account for the relatively large uncertainty in the isotope composition of the terrestrial contaminant and they do not incorporate the comparatively small mass spectrometric errors.

The results of Table 3 show that the total Pb contents of the iron meteorites required correction for about 1–95% of terrestrial contamination. Large corrections were particularly necessary for samples with low primordial Pb concentrations. In these cases, the total uncertainties that are quoted for the ^{204}Pb/^{203}Tl ratios are dominated by the correction for terrestrial Pb contamination. The errors reported for the ^{204}Pb/^{203}Tl ratios, however, also include: (1) the uncertainty of the Tl blank correction (1.0 ± 0.5 pg), and (2) the within-run errors of the mass spectrometric concentration measurements, which are about ± 0.2 to $\pm 2‰$, for Pb and ± 0.5 to $\pm 20‰$ for Tl, depending on sample size and elemental concentration. It is notable that all particularly critical samples (e.g., the Toluca and Canyon Diablo metals) required corrections of less than 10–50% for the terrestrial Pb contamination.

Table 3
Pb and Tl concentrations and Pb and Tl isotope compositions of the iron meteorite samples

Sample	Group	Sample weight[a] (g)	ε^{205}Tl	^{204}Pb/^{203}Tl	^{206}Pb/^{204}Pb (calculated)	^{207}Pb/^{204}Pb (calculated)	^{208}Pb/^{204}Pb (calculated)	Fraction of primordial Pb[b]	^{204}Pb[c] (pmol/g)	^{203}Tl (pmol/g)
Metals										
Canyon Diablo	IAB	8.43	-1.8 ± 1.0	0.675 ± 0.040	12.53 ± 0.13	12.29 ± 0.13	32.59 ± 0.13	0.54	1.57	2.32
Toluca AB	IAB	5.96	14.2 ± 2.0	50.4 ± 2.3	9.86 ± 0.02	10.63 ± 0.02	30.01 ± 0.02	0.91	5.10	0.101
Toluca C	IAB	7.7	16.7 ± 1.5	58.6 ± 1.0	9.70 ± 0.01	10.54 ± 0.01	29.85 ± 0.01	0.94	8.39	0.143
Toluca Ir-30m	IAB	6.32	11.9 ± 1.5	53.2 ± 2.2	9.554 ± 0.007	10.447 ± 0.008	29.714 ± 0.008	0.96	3.82	0.072
Toluca Ir-30n-1	IAB	5.05	-1.4 ± 1.0	0.131 ± 0.003	11.11 ± 0.06	11.41 ± 0.07	31.21 ± 0.06	0.72	3.15	24.1
Toluca Ir-30n-2	IAB	5.29	-2.7 ± 1.0	0.471 ± 0.011	11.05 ± 0.06	11.37 ± 0.06	31.16 ± 0.06	0.73	4.29	9.11
Toluca USNM 75	IAB	7.37	23.3 ± 1.5	76.5 ± 4.3	9.85 ± 0.02	10.63 ± 0.02	30.00 ± 0.02	0.91	3.40	0.044
Murphy USNM 557	IIAB	21.72	0.9 ± 3.0	18.9 ± 7.0	16.22 ± 0.35	14.56 ± 0.32	36.14 ± 0.35	0.15	0.100	0.0053
Navajo USNM 5601	IIAB	22.49	-1.6 ± 2.0	0.30 ± 0.30	17.37 ± 0.36	15.28 ± 0.33	37.26 ± 0.36	0.04	0.009	0.029
Mount Edith USNM 528	IIIAB	36.42	16.1 ± 3.0	12.0 ± 5.7	16.66 ± 0.39	14.84 ± 0.34	36.57 ± 0.38	0.11	0.061	0.0051
Grant	IIIAB	14.88	18.9 ± 3.0	9.3 ± 1.0	12.64 ± 0.13	12.36 ± 0.13	32.69 ± 0.13	0.52	0.111	0.012
Mundrabilla A	An	11.2	29.9 ± 1.0	14.2 ± 0.1	9.80 ± 0.02	10.60 ± 0.02	29.96 ± 0.02	0.92	7.60	0.536
Mundrabilla B	An	12.3	29.1 ± 1.0	10.2 ± 0.1	9.99 ± 0.02	10.72 ± 0.02	30.13 ± 0.02	0.89	11.2	1.10
Sulfides										
Canyon Diablo USNM 676 A	IAB	2.32	-19.0 ± 1.0	31.2 ± 0.06	9.364 ± 0.002	10.329 ± 0.002	29.531 ± 0.002	0.99	242	7.76
Canyon Diablo USNM 676 B	IAB	1.29	-6.4 ± 1.0	55.4 ± 0.3	9.461 ± 0.005	10.389 ± 0.005	29.625 ± 0.005	0.98	133	2.40
Toluca USNM 75	IAB	2.77	-12.9 ± 1.0	11.4 ± 0.1	9.627 ± 0.010	10.492 ± 0.011	29.784 ± 0.010	0.95	64.9	5.71
Toluca Ir-30m	IAB	1.43	10.8 ± 1.0	12.6 ± 0.1	9.334 ± 0.001	10.311 ± 0.001	29.502 ± 0.001	>0.99	502	39.9
Toluca Ir-30a[d]	IAB	6.86	-6.0 ± 1.0	9.75 ± 0.03	9.433 ± 0.004	10.372 ± 0.004	29.598 ± 0.004	0.98	8.12	0.832
Grant	IIIAB	0.818	-3.4 ± 2.0	0.78 ± 0.15	15.33 ± 0.29	14.02 ± 0.27	35.29 ± 0.29	0.24	0.529	0.674
Mundrabilla	An	1.47	24.2 ± 2.0	0.57 ± 0.57	—	—	—	0.5 ± 0.5[e]	0.235	0.409
Bulk silicate Earth			-2.0 ± 0.5[g]	2.0					10.3[f]	5.1[f]

The absolute ^{204}Pb and ^{203}Tl concentrations have uncertainties of about ±5–10%, mainly from uncertainties in the weights of the leached samples and the solution aliquots. The uncertainties of the ^{204}Pb/^{203}Tl ratios reflect the mass spectrometric precision and corrections for blank and terrestrial (Pb) contamination. The uncertainties for the Tl isotope compositions represent the 2σ reproducibilities of standard measurements conducted at ion beam intensities similar to those obtained for the respective samples (see text for details). The Pb isotope compositions are calculated based on the measured ^{207}Pb/^{206}Pb and ^{208}Pb/^{206}Pb isotope ratios for the isotope dilution runs.

[a] Weight after leaching.

[b] Defined as fraction of primordial Pb compared to total measured (= primordial + terrestrial Pb) present in the samples.

[c] Concentration corrected for terrestrial contamination.

[d] Sample Toluca Ir-30a consisted of metal, with a large sulfide inclusion trapped in the center.

[e] Due to the low Pb content of this sample and the high degree of contamination, the calculations did not yield reasonable results. This sample was therefore assigned a Pb concentration equivalent to half the measured (= uncorrected) Pb concentration, with an uncertainty of ±100%.

[f] Recalculated from McDonough and Sun (1995).

[g] See Nielsen et al. (2005, 2006).

2.5. Statistics and data handling

All isochron calculations were performed with the Isoplot program of Ken Ludwig (Berkeley Geochronology Center) and assuming a reference value of $^{205}Tl/^{203}Tl = 2.3871$ for the NIST SRM 997 Tl isotope standard.

3. Results and discussion

3.1. General features

The Tl isotope compositions as well as Pb and Tl concentrations have been determined for metal and sulfide phases from iron meteorites of groups IAB, IIAB, and IIIAB and the unclassified iron Mundrabilla (Table 3). It can be seen that the samples display a broad range of primordial ^{204}Pb and ^{203}Tl contents. In general terms, the concentrations are similar to those reported in the latest published Pb–Tl study of iron meteorites (Chen and Wasserburg, 1994b). All sulfides except one display higher Pb and Tl concentrations than the co-existing metals, which is also expected (Chen and Wasserburg, 1994b). However, it is also apparent that neither Pb nor Tl show evidence of simple metal–sulfide partitioning, as large variations in absolute concentrations exist even for different metal fragments of the same meteorite (Table 3). This large spread in ^{204}Pb and ^{203}Tl abundances is probably due to the inhomogeneous distribution of micro-phases with high concentrations of Tl, Pb, and other (metal) incompatible trace elements, as predicted by Jones et al. (1993) and it is analogous to the behavior observed for Ag in the metal phase of iron meteorites (Chen and Wasserburg, 1990). The exact chemical composition of these phases is unknown. Furthermore, despite a broad range of values, there is no systematic difference in Pb/Tl between sulfides and metal. Among co-existing sulfide–metal pairs, however, the Pb/Tl ratios are normally somewhat lower in the sulfides.

The Tl isotopic compositions are also extremely variable, with results from $\varepsilon^{205}Tl = -19 \pm 1$ for a Canyon Diablo sulfide to $\varepsilon^{205}Tl = +29 \pm 1$ for Mundrabilla metal. Despite of its high mass, Tl exhibits significant low temperature stable isotope effects in terrestrial samples (Rehkämper and Halliday, 1999; Rehkämper et al., 2002, 2004; Nielsen et al., 2004a, 2005). The ~50 ε-unit range found in iron meteorites is, however, far greater than the Tl isotope variations that have been established for any environment on Earth, as can be seen from Fig. 1, which compares results for various terrestrial and extraterrestrial materials. The largest single stable isotope effect identified so far is the ~20 ε-unit fractionation between seawater and ferromanganese marine sediments (Rehkämper et al., 2002). Evidence for stable isotope variations of Fe and Ag has been found in iron meteorite sulfides (Williams et al., 2004; Woodland et al., 2005) but these are sub-permil level effects, which are much smaller than the present Tl

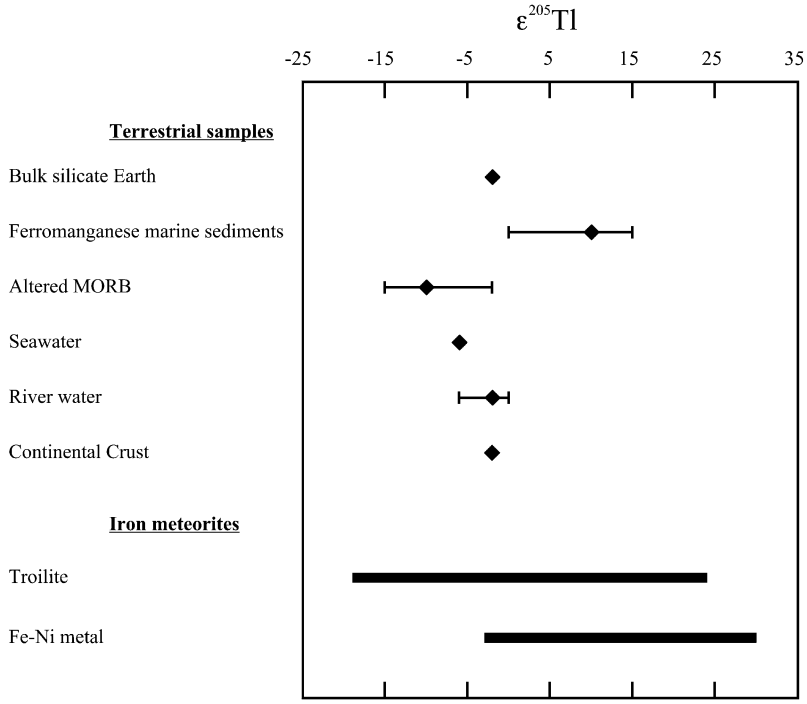

Fig. 1. Thallium isotope compositions of various terrestrial reservoirs compared with the range of $\varepsilon^{205}Tl$ values determined for iron meteorites. The terrestrial data are global averages and the error bars denote the range of values measured for the respective samples. It is evident that the iron meteorites exhibit a larger variation in $\varepsilon^{205}Tl$ than the terrestrial samples. This suggests that at least some of the isotopic variation recorded by iron meteorites is due to decay of ^{205}Pb to ^{205}Tl. Terrestrial Tl isotope compositions are from Nielsen et al. (2004a,b, 2005, 2006) and Rehkämper et al. (2002, 2004).

isotope variations. Alternative mechanisms for producing variations in the $^{205}Tl/^{203}Tl$ isotope ratio, such as cosmogenic spallation or neutron capture, are not expected to be important due to the high mass of Tl and the relatively small cross-sections of ^{203}Tl, ^{205}Tl, and ^{204}Pb, which would be the principle isotopes capable of producing effects from neutron capture. This strongly suggests that at least some of the Tl isotope variability observed for iron meteorites may be the result of radioactive decay of formerly live ^{205}Pb to ^{205}Tl.

In order to evaluate this hypothesis, the results are plotted in $\varepsilon^{205}Tl$ versus $^{204}Pb/^{203}Tl$ isochron diagrams (Figs. 2a and b). Numerous analyses were performed for the group IAB iron Toluca, and metal fragments of this meteorite display a large range of Tl isotope compositions, with values from $\varepsilon^{205}Tl = -2.7$ to $+23.3$, that correlate linearly with $^{204}Pb/^{203}Tl$, providing evidence for the former existence of live ^{205}Pb. In the following, we first discuss the data of Toluca and other meteorites that display similar results.

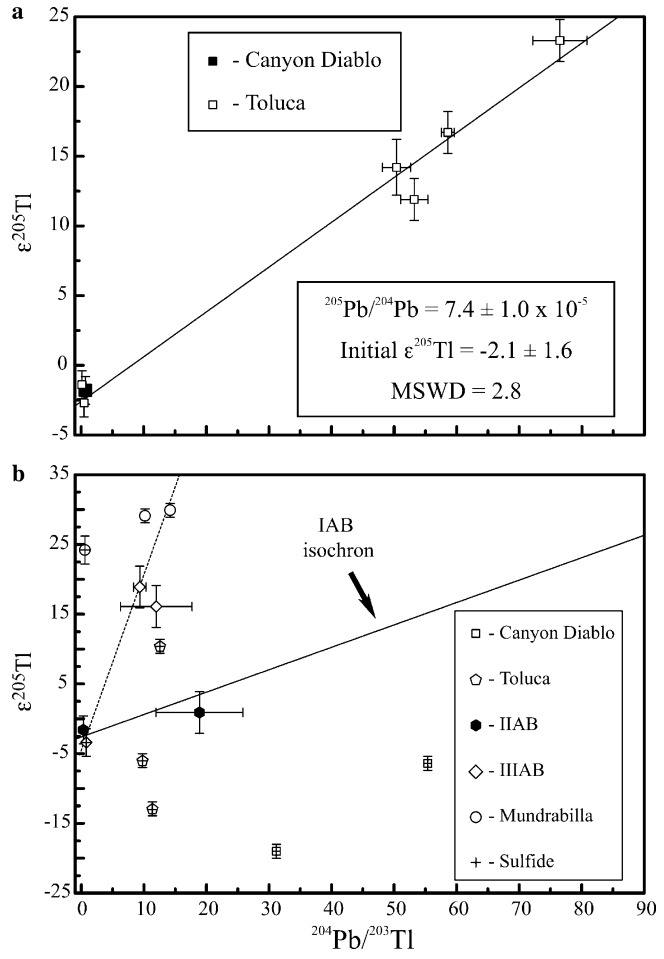

Fig. 2. Pb–Tl isochron diagrams for iron meteorites. (a) Results for metal samples of IAB irons. Six metal fragments of Toluca and a single metal from Canyon Diablo precisely define the IAB iron meteorite isochron. (b) Results for troilites from Toluca and Canyon Diablo as well as data for metal and sulfide samples of IIAB and IIIAB iron meteorites and the anomalous iron Mundrabilla. The IAB isochron (full line) is shown for reference and a potential IIIAB isochron (see text) is denoted by the dotted line.

Subsequently, we address the more complex results obtained for sulfides and metal samples from other meteorites, which appear to reflect the superimposed effects of isotope fractionation and radiogenic addition of ^{205}Tl.

3.2. IAB metal isochron

Seven different metal samples from non-magmatic IAB iron meteorites have been analyzed. The ^{204}Pb concentrations of six separate metal fragments of Toluca range between about 3 and 8 pmol/g, whereas the ^{203}Tl contents are found to vary by more than two orders of magnitude between about 0.04 and 24 pmol/g (Table 3). Consequently, the $^{204}Pb/^{203}Tl$ ratios are very variable, and these data yield an excellent correlation with the Tl isotope compositions (Fig. 2a). In principle, these results could be explained in any one of three following ways:

1. The variations reflect stable isotope fractionation.
2. The correlation is a mixing line that is generated by two distinct endmembers.
3. The data define an isochron produced by radioactive decay of ^{205}Pb.

As Tl only has two isotopes, it is very difficult to exclude that the Tl isotope variations observed for the IAB metal samples are due to stable isotope fractionations. However, if this is the case there is no logical reason why the isotopic compositions should correlate with the Pb/Tl ratios. Stable isotope effects are likely to play a role for some of the other samples and the origin of these and potential effects on isochron relationships are discussed in more detail in the following section.

Mixing between endmembers is a simpler hypothesis to evaluate. It is conceivable that the Toluca metal isochron represents a mixing line between a Tl-rich component with isotopically normal Tl ($\varepsilon^{205}Tl \approx -2$) and a Tl-poor component (presumably the metal), which displays $\varepsilon^{205}Tl$ values of about +25 or above. There are two different mechanisms by which such a mixing line could be produced. First, it is possible that the mixing line reflects terrestrial contamination because the BSE has a $^{204}Pb/^{203}Tl$ ratio and $\varepsilon^{205}Tl$ value (Table 3) that is indistinguishable from the Tl-rich component. The correlation of Fig. 2a would then represent a mixing line that connects the pristine Tl isotope composition of Toluca ($\varepsilon^{205}Tl \geqslant 25$) with a terrestrial contaminant. This model can be further evaluated by determining the extent of terrestrial Tl contamination. An independent measurement of the contamination is not available but its extent can be estimated by mass balance based on a reasonable assumption of the "true" Tl isotope composition of the Toluca metal. For simplicity, the calculations assume a pristine Toluca value of $\varepsilon^{205}Tl = 25$ but the results are effectively identical even for a value of $\varepsilon^{205}Tl = 100$. The extent of terrestrial contamination calculated for Pb (Table 3) and Tl are then combined and this provides an estimate for the $^{204}Pb/^{203}Tl$ ratio of the

Table 4
Estimates for the $^{204}Pb/^{203}Tl$ ratio of the hypothetical terrestrial contaminant postulated for the Toluca metal samples

Toluca metal sample	Fraction of terrestrial Tl contamination[a]	Calculated $^{204}Pb/^{203}Tl$ ratio of the contaminant
Metal AB	0.40	12.4
Metal C	0.31	12.2
Ir-30m	0.48	4.6
Ir-30n-1	0.98	0.05
Ir-30n-2	1	0.17
USNM 75	0.06	119

[a] The calculation assumes that the uncontaminated Toluca metal and the terrestrial contaminant are characterized by $\varepsilon^{205}Tl = 25$ and -2, respectively.

hypothetical contaminant that may have been added to each sample (Table 4). It is evident, that these calculations yield terrestrial contaminants that display widely varying $^{204}Pb/^{203}Tl$ ratios of between 0.05 and 119. This range of values is reduced if a higher value for the true Tl isotope composition of the Toluca metal is assumed, but even a value of $\varepsilon^{205}Tl = 100$ still requires $^{204}Pb/^{203}Tl$ ratios of between 0.05 and 10. Given that a potential contaminant is likely to display only a relatively limited variation of Pb/Tl ratios, it appears very improbable that terrestrial contamination generated the observed correlation of Tl isotope compositions with $^{204}Pb/^{203}Tl$ (Fig. 2a).

The second potential means of producing a pseudo isochron is by mixing of two discrete mineral phases that are present in the iron meteorite itself. This model requires that two endmembers with extremely different Tl isotope composition were generated in a single and once molten object. This is an unlikely scenario, unless the endmembers were produced by the decay of ^{205}Pb, which, of course, means the isochron is still valid. Furthermore, it is clear that the Tl isotope compositions display a relatively poor correlation when plotted against 1/Tl (Fig. 3) rather than $^{204}Pb/^{203}Tl$ (Fig. 2a). Mixing between two discrete mineral phases should, however, produce an identical or better correlation in $\varepsilon^{205}Tl$–1/Tl space because the Pb concentration has no effect on the Tl isotope composition in this scenario. This is clearly not the case and it is therefore reasonable to conclude that mixing is not a viable explanation for the Toluca correlation line.

The most straightforward interpretation of the Tl isotope variations in the Toluca metal samples is therefore that the results define an isochron, which records the timing of crystallization of a metal phase from a sulfur-rich metallic liquid. A single metal sample from the Canyon Diablo (IAB) iron meteorite confirms the Toluca results and together the data define a "IAB isochron" corresponding to initial values of $(^{205}Pb/^{204}Pb)_{IAB,0} = (7.4 \pm 1.0) \times 10^{-5}$ and $\varepsilon^{205}Tl_{IAB,0} = -2.1 \pm 1.6$ (Fig. 2a). Assuming this is indeed the correct interpretation, the initial abundance of ^{205}Pb in the solar system, $(^{205}Pb/^{204}Pb)_{SS,0}$, can be calculated from these results, if the time interval between the formation of the first refractory solids (t_0) and the crystallization of the IAB metal phase is known.

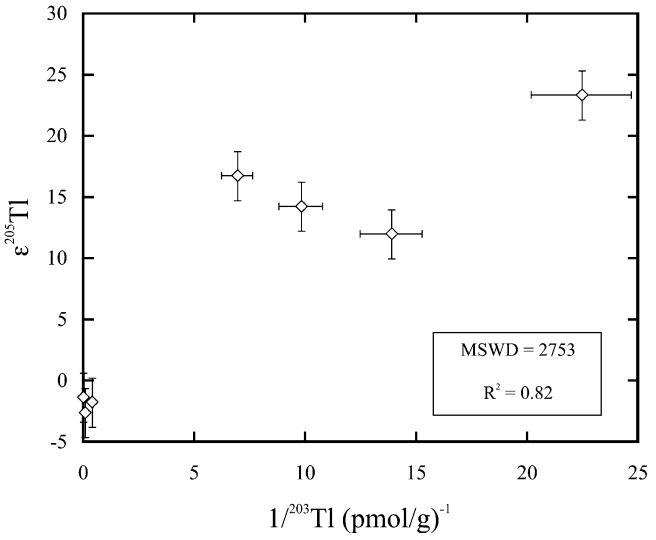

Fig. 3. Thallium isotope compositions of the IAB metal samples plotted against 1/Tl concentration. If the isotope compositions reflect simple mixing of Tl derived from two discrete mineral phases, this should generate a correlation in this diagram that is superior to the one seen in Fig. 2a ($\varepsilon^{205}Tl$ versus $^{204}Pb/^{203}Tl$). A comparison of the MSWD values clearly shows that this is not the case.

The I–Xe chronometer has been used to date the cooling of silicate inclusions of Toluca and other IAB meteorites and this provides ages of 10–20 Myr after t_0 (Niemeyer, 1979; Pravdivtseva and Hohenberg, 2000). Application of this time difference yields $(^{205}Pb/^{204}Pb)_{SS,0}$ ratios of $(1.0–2.1) \times 10^{-4}$. Of course, the I–Xe and Pb–Tl chronometers may not necessarily record the same event. Based on evidence from Ar–Ar, Rb–Sr, and ^{147}Sm–^{143}Nd chronometry, it has been inferred that the IAB iron meteorites have a complex thermal history with isotopic resetting occurring up to several hundred million years after solar system formation (Bogard et al., 2005). As ^{205}Pb would have been essentially extinct at the time of any late events, such protracted episodes of resetting cannot be recorded by Pb–Tl isochrons. The closure temperature of the I–Xe chronometer is probably higher than 1000 °C (Burkland et al., 1995) whereas it is unknown for the Pb–Tl system. The cooling rate of Toluca and other IAB irons with low Ni concentrations have been determined at about 25–30 °C/Myr (Herpfer et al., 1994; Saikumar and Goldstein, 1988), such that the Pb–Tl closure temperature would need to be <800 °C to create a significant age difference between the I–Xe and Pb–Tl systems.

3.3. IAB troilite nodules and effects of stable isotope fractionation

3.3.1. Stable isotope fractionation in troilite nodules

The Tl isotope data obtained for troilite nodules of both Toluca and Canyon Diablo are not in accord with the simple isochron relationships exhibited by the metals (Fig. 2b) because all sulfides except one plot at lower $\varepsilon^{205}Tl$ values for a given $^{204}Pb/^{203}Tl$ ratio. In studies of

extinct radionuclides it has been standard practice to use the least radiogenic isotope ratio measured as the best approximation of the solar system initial. In this case, the most ^{205}Tl-depleted value of $\varepsilon^{205}\mathrm{Tl} = -19$, obtained for a sulfide from Canyon Diablo, would be assumed to provide a good estimate of the initial Tl isotope composition of the solar system ($\varepsilon^{205}\mathrm{Tl}_{SS,0}$). This assumption must be questioned for the ^{205}Pb–^{205}Tl decay system because Tl possesses only two isotopes, such that there is no straightforward way to distinguish between isotopic variations from the decay of ^{205}Pb and mass dependent stable isotope effects. With regard to the present data there are, furthermore, a number of constraints which indicate that the most unradiogenic Tl isotope composition of $\varepsilon^{205}\mathrm{Tl} = -19$ is unlikely to be representative of, or similar to, $\varepsilon^{205}\mathrm{Tl}_{SS,0}$.

First, if the least radiogenic sulfide has a Tl isotope composition that best approximates the initial value of the solar system, then all metal samples would plot above any reasonable isochron constructed through this sulfide. This would also imply that the metal phase has been isotopically reset preferentially to the troilite. This conclusion, however, is inconsistent with evidence from Ag and Os isotope studies, which have shown that isotopic resetting occurs more readily for sulfides than for the metal phase (Chen and Wasserburg, 1990, 1996; Shen et al., 1996; Woodland et al., 2005).

Second, it is very difficult to understand how some metals of iron meteorites evolved from a solar system initial of $\varepsilon^{205}\mathrm{Tl}_{SS,0} \leqslant -19$ to ε^{205}Tl values of up to +30 (Mundrabilla), considering the relatively low ^{204}Pb/^{203}Tl ratios measured for these samples (Table 3) and taking into account that all present and previous Tl isotope data obtained for meteorites imply that $(^{205}\mathrm{Pb}/^{204}\mathrm{Pb})_{SS,0} < 3 \times 10^{-4}$ (Huey and Kohman, 1972; Chen and Wasserburg, 1987). Fig. 4 is a plot of the calculated $(^{205}\mathrm{Pb}/^{204}\mathrm{Pb})_{SS,0}$ values plotted versus the corresponding ^{204}Pb/^{203}Tl ratios, which are consistent with a present day $\varepsilon^{205}\mathrm{Tl} = 30$ for the Mundrabilla metal and $\varepsilon^{205}\mathrm{Tl}_{SS,0} = -19$, as defined by the most unradiogenic Canyon Diablo sulfide. It can be seen that this large spread in Tl isotopic compositions requires either $(^{205}\mathrm{Pb}/^{204}\mathrm{Pb})_{SS,0} > 8 \times 10^{-4}$, about a factor of 3–4 higher than the upper limit for $(^{205}\mathrm{Pb}/^{204}\mathrm{Pb})_{SS,0}$ as defined by the Toluca isochron and previous studies (Huey and Kohman, 1972; Chen and Wasserburg, 1987), or ^{204}Pb/^{203}Tl > 40–60, which is about a factor 3–4 higher than the largest ^{204}Pb/^{203}Tl ratio measured for Mundrabilla.

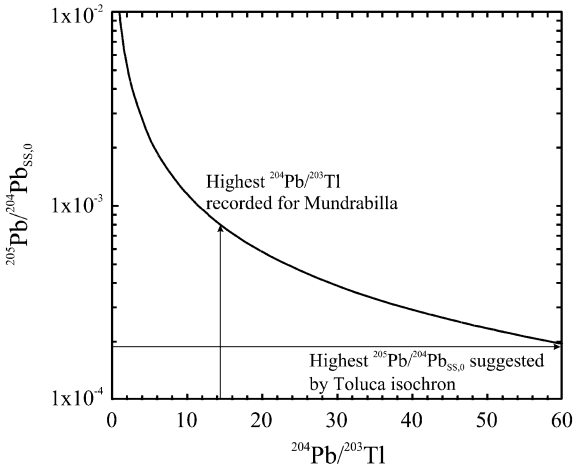

Fig. 4. Plot of ^{204}Pb/^{203}Tl ratios and $^{205}\mathrm{Pb}/^{204}\mathrm{Pb}_{SS,0}$ values required to explain the evolution of the Mundrabilla iron meteorite from an assumed initial solar system $\varepsilon^{205}\mathrm{Tl}_{SS,0} = -19$ to the current value of $\varepsilon^{205}\mathrm{Tl} = +30$. If bulk Mundrabilla is characterized by a ^{204}Pb/^{203}Tl ratio akin to the highest value measured for this meteorite ($^{204}\mathrm{Pb}/^{203}\mathrm{Tl} \approx 14$), the isotopic evolution would require $^{205}\mathrm{Pb}/^{204}\mathrm{Pb}_{SS,0} > 8 \times 10^{-4}$. If it is assumed that $^{205}\mathrm{Pb}/^{204}\mathrm{Pb}_{SS,0} < 1.9 \times 10^{-4}$, as calculated from the Toluca isochron, then bulk Mundrabilla would need to be characterized by $^{204}\mathrm{Pb}/^{203}\mathrm{Tl} > 60$.

Not only is the idea that all of the Tl isotopic effects reflect ^{205}Pb decay inconsistent with the iron meteorite data, it is also very hard to reconcile with the Tl isotopic composition of the bulk silicate Earth. The silicate Earth (Nielsen et al., 2005, 2006) and the chondrite Allende (Rehkämper and Halliday, 1999) have ε^{205}Tl values that are broadly similar to the initial Tl isotopic composition of the solar system, as defined by the Toluca metals. This is fully consistent with $(^{205}\mathrm{Pb}/^{204}\mathrm{Pb})_{SS,0} < 3 \times 10^{-4}$. In contrast, there is no explanation that readily predicts similar values for the BSE and bulk chondrites if $(^{205}\mathrm{Pb}/^{204}\mathrm{Pb})_{SS,0} > 8 \times 10^{-4}$. Finally, a $(^{205}\mathrm{Pb}/^{204}\mathrm{Pb})_{SS,0}$ value of less than 3×10^{-4} is consistent with the results of nucleosynthetic modeling, as discussed below.

Based on this, it is concluded that a process other than radiogenic ingrowth has affected the Tl isotopic compositions of the sulfides. By analogy with observations made for Fe (Williams et al., 2004; Weyer et al., 2005), Ag (Woodland et al., 2005), and Ni (Quitte et al., 2005) isotopes, this process is most likely some form of stable isotope fractionation, which appears to preferentially affect the sulfide inclusions.

For the ^{107}Pd–^{107}Ag system, the sulfides generally plot near the low-Pd/Ag origin of isochrons that are defined by metal fragments and in most cases they exhibit an excess of radiogenic ^{107}Ag. This excess was interpreted to reflect diffusion of radiogenic Ag from the metal phase (with very high Pd/Ag) to associated troilite inclusions, either during slow cooling or secondary heating from shock or thermal metamorphism (Chen and Wasserburg, 1990). Only one of the sulfides from the IAB irons analyzed in the present study (sample Ir-30m, Table 3), however, displays an excess of radiogenic Tl that can be readily explained by simple redistribution. All other troilites of Toluca and Canyon Diablo have ε^{205}Tl values that are significantly less radiogenic than the metal samples (Fig. 2b). This result can reflect late redistribution of Tl only if diffusion is accompanied by isotope fractionation, and this may arise from the preferential transport of the lighter ^{203}Tl isotope, as would be expected for kinetic isotope fractionation.

3.3.2. Modeling of diffusive stable Tl isotope fractionation in troilite

If the sulfides have received a significant amount of isotopically light Tl from the metal phase through diffusion

and isotope fractionation, the mass balance of this process could potentially disturb the isochron relationships exhibited by the metal samples. In a worst-case scenario this effect could be responsible for the entire range of Tl isotope compositions observed for the Toluca metals. Such a situation could occur if the relative diffusivities of Pb and Tl are constant, such that the progressive depletion and isotope fractionation of Tl in the metal is accompanied by a systematic change in the Pb/Tl ratio.

To investigate whether isotopically fractionated sulfides can co-exist with relatively undisturbed metals, simple model calculations were performed that apply realistic values for the Tl concentrations and mass fractions of sulfide and metal present, as well as reasonable isotope fractionation factor, α, of 0.9970 and 0.9985. The kinetic isotope fractionation generated by diffusion is given by $\alpha = D_1/D_2 = (m_2/m_1)^{\beta}$, where D_i denotes the diffusivity of an isotope i of mass m_i. For self-diffusion in a gas, the isotope fractionation is characterized by $\beta = 0.5$, which is equivalent to a fractionation factor for ^{203}Tl and ^{205}Tl of $\alpha_{Tl} = 0.9951$. For condensed phases the exponent β is smaller, silicate melts displaying $\beta \approx 0.1$ (Tsuchiyama et al., 1994). As no experimental data are available that constrain the isotope fractionation from diffusion of Tl between molten or solid sulfides and Fe–Ni metal, we have arbitrarily chosen intermediate α_{Tl} values of 0.9970 and 0.9985, which are equivalent to $\beta \approx 0.3$ and 0.15, respectively. The results of these calculations (Fig. 5) demonstrate that isotopic shifts of −10 to −15 ε^{205}Tl-units can be achieved for the sulfides, without disturbing the Tl isotope composition and concentration of the associated metal by more than 2 ε^{205}Tl and ~10%, respectively, and this is similar to the typical analytical uncertainties of our measurements (Table 3). It is important to note that the results are dependent on the initial Tl concentrations and relative modal abundances of metal and troilite. For example, an increase in the modal abundance of sulfide by a factor of 10 from 0.5 to 5 g of troilite per 100 g of metal, limits the isotopic shifts that can be achieved for the sulfides without significantly (>2 ε-unit) disturbing the metal phase to only about −3 to −4 ε^{205}Tl-units. The data for some of the sulfides measured here (Table 3) are in accord with such a scenario. The best estimate for the average S content of Toluca yields a value of about 7 mg/g (Buchwald, 1975) corresponding to a maximum troilite abundance (assuming no sulfur in the metal) of ~2 g per 100 g of metal. Trolite nodules are, however, not evenly distributed in iron meteorites. As a result, one would expect different nodules to have variable Tl isotope compositions, and this is consistent with our current results.

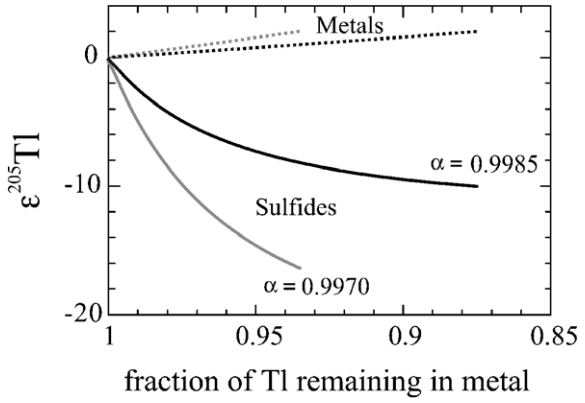

Fig. 5. Results of model calculations that illustrate the effect of isotope fractionation associated with Tl diffusion from the metal to the troilite phase of iron meteorites. The two solid curves show the calculated ε^{205}Tl data of sulfides for two different values of the isotope fractionation factor, α, as a function of the fraction of Tl remaining in the accompanying metal. The results for the respective metal phases are denoted by the dashed lines. The calculations are for a system consisting of 100 g of metal with $[Tl]_0 = 0.5$ pmol/g and 0.5 g sulfide with $[Tl]_0 = 5$ pmol/g. Both phases are initially characterized by $\varepsilon^{205}Tl = 0$. It is evident that this process can generate sulfides with low ε^{205}Tl, without changing the isotope compositions of the accompanying metals by more than +2 ε^{205}Tl. The Tl concentrations of the sulfides are also increased, by about a factor of 2–3.

Irrespective of these apparent consistencies, the fractionation effects of the model can also significantly alter the Tl isotope composition of the metal phase. In principle, it is therefore conceivable that the processes, which are inferred to have generated the fractionated Tl isotope signatures of the sulfides, also affected the metal. However, considering that the IAB sulfides display a large range of ε^{205}Tl values and Pb/Tl ratios, it seems unlikely that the tight correlation observed for the corresponding metal samples in the isochron diagram of Fig. 2a was appreciably altered by kinetic isotope effects. It is therefore reasonable to assume that the IAB metal samples were essentially unaffected by the diffusion-related processes that are inferred to have produced the fractionated Tl isotope compositions of the sulfides.

3.4. Other iron meteorites

Data also were obtained for the IIAB magmatic irons Navajo (USNM 5601) and Murphy (USNM 557). Only samples of the metal phase were available for these meteorites and they show Pb and Tl concentrations that are significantly lower than those of the IAB metals (Table 3). Due to these lower abundances there are large errors associated with both the concentration and the Tl isotope measurements. However, both samples plot on the IAB metal isochron within error (Fig. 2b), which indicates that IAB and IIAB irons probably have similar crystallization ages.

A very different pattern is discernable for metals of the IIIAB irons Grant and Mount Edith (USNM 528). These samples have low Pb and Tl abundances, similar to those observed for the IIAB irons, but the Tl isotope compositions are displaced to values about 15 ε^{205}Tl-units above the IAB metal isochron (Table 3 and Fig. 2b). A troilite nodule from Grant follows the pattern observed for the IAB sulfides, whereby high Pb and Tl concentrations are combined with a markedly lower ε^{205}Tl compared to the corresponding metal sample.

Even more extreme Tl isotope compositions were obtained for the Mundrabilla iron meteorite, which has been classified as an anomalous IIICD iron (Choi et al., 1995).

Two metal fragments and one troilite nodule yielded ε^{205}Tl values of +24 to +30, and these are the highest values observed in this study. The Mundrabilla metals are furthermore unusual because: (1) they have the highest Pb and Tl contents of all metals analyzed in this study, and (2) these abundances are even higher than those of the co-existing troilite, which is opposite to the relationship found for all other metal–sulfide pairs (Table 3).

Taken at face value, the data for the IIIAB metal and sulfide samples could be interpreted as a parent body isochron with a slope that defines an initial $^{205}Pb/^{204}Pb$ of $(6.2 \pm 1.2) \times 10^{-4}$. The comparison of this result to the initial value of $^{205}Pb/^{204}Pb \approx 7.4 \times 10^{-5}$ obtained for the IAB meteorites then implies that the IIIAB's crystallized about 46 ± 5 Myr prior to the IAB (and IIAB) irons. This is an implausible conclusion for two reasons. Firstly, the IIAB and IIIAB irons have very similar Pd–Ag ages of crystallization (Chen and Wasserburg, 1996). Second, recently published Ag isotope data for metal samples of Toluca and Canyon Diablo (Carlson and Hauri, 2001; Woodland et al., 2005) indicate an initial $^{107}Pd/^{108}Pd$ of $(9.1 \pm 5.5) \times 10^{-6}$ for the IAB irons, which compares with 1.7×10^{-5} for the IIIAB iron meteorites (Chen and Wasserburg, 1996), and this is equivalent to a time difference of only 1–15 Myr. Thus, the Tl isotope composition of the Grant troilite is also likely to reflect complex open-system behavior as is found for the other sulfides. The following discussion therefore focuses on the results obtained for metal samples.

Based on the assumption that the crystallization of the IIIAB irons does not predate the IAB metals by more than 15 Myr, the IIIAB iron meteorites are likely to have had initial $\varepsilon^{205}Tl_0$ values of about +10, or larger. The similar Tl isotope compositions of the two Mundrabilla metal fragments furthermore suggest that this meteorite was characterized by an initial $\varepsilon^{205}Tl_0$ of greater than +20 (Fig. 2b). Compared to the IAB and IIAB irons, the IIIAB's and Mundrabilla thus have significantly more radiogenic (or isotopically heavier) initial Tl isotope compositions. It is improbable that these differences reflect the inhomogeneous distribution of Tl isotopes or ^{205}Pb in the early solar system, high temperature stable isotope fractionations that occurred during metal–silicate differentiation, or core crystallization, because such effects are expected to be relatively small in iron meteorites. The most likely explanation for the differences in $\varepsilon^{205}Tl_0$ is therefore either enhanced radiogenic ingrowth of ^{205}Tl in a parent body or core characterized by high Pb/Tl prior to core crystallisation or stable isotope effects that were generated by partial evaporation and/or condensation of highly volatile Tl.

Assuming an initial $(^{205}Pb/^{204}Pb)_{SS,0}$ of 1.5×10^{-4} and 15 Myr of parent body evolution, an excess of +10 ε^{205}Tl for the IIIAB's can be generated by radiogenic decay only for bulk $^{204}Pb/^{203}Tl$ ratios of ~32. This is about a factor of 3 higher than the $^{204}Pb/^{203}Tl$ ratios determined for IIIAB iron meteorites in this study. Furthermore, Pd–Ag isotope studies have shown that IIAB, IIIAB, and IVA irons all crystallized within about 5 Myr of each other (Chen and Wasserburg, 1996). If the Pb–Tl and Pd–Ag chronometers record the same event, as would be expected, then it appears unlikely that the IIIAB parent body could have experienced 15 Myr of radiogenic ingrowth prior to core crystallization. For Mundrabilla, the initial $\varepsilon^{205}Tl_0$ is even higher. The lack of resolvable Ag isotope effects for this meteorite indicates that the crystallization of the metal may have occurred late (Chen and Wasserburg, 1996). However, the inferred initial excess of >+20 ε^{205}Tl still requires a bulk $^{204}Pb/^{203}Tl$ ratio of at least ~30, which is not supported by the $^{204}Pb/^{203}Tl$ ratios determined for Mundrabilla in this study. Based on this, it is likely that the high initial $\varepsilon^{205}Tl_0$ values of the IIIAB iron meteorites and Mundrabilla reflect not only a parent body with high Pb/Tl but also, at least in part, the effects of isotope fractionations that occurred as the result of volatile loss from or redistribution on primitive or differentiated planetesimals. Supporting evidence for such a mechanism has been found in the Cd isotopic compositions of ordinary chondrites (Wombacher et al., 2003).

4. Implications

4.1. Astrophysical implications of the solar system initial $^{205}Pb/^{204}Pb$

The inferred value of $(^{205}Pb/^{204}Pb)_{SS,0} \approx 1.5 \times 10^{-4}$ can be compared with predictions based on stellar models of proposed s-process nucleosynthetic sites. Astrophysical studies indicate that Wolf-Rayet (WR) and asymptotic giant branch (AGB) stars are feasible sites of s-process nucleosynthesis (Wasserburg et al., 1994; Arnould et al., 1997), as both feature suitable neutron fluxes and they are also known to expel large amounts of material into the interstellar medium (ISM). Wolf-Rayet stars are large (~20 solar masses), short-lived objects that shed mass at a rapid rate and may eventually evolve into a supernova. In contrast, AGB stars are relatively common low mass stars (<8 solar masses) in which fusion reactions and intermittent thermal pulses redistribute new nuclides and neutrons as by-products. Nucleosynthetic production calculations for both star types have utilized dilution factors for the expelled material that are scaled to achieve $^{107}Pd/^{108}Pd = 2 \times 10^{-5}$, as this approximates the initial abundance of ^{107}Pd determined for the oldest magmatic irons (Chen and Wasserburg, 1996).

The production calculations for WR stars yield $^{205}Pb/^{204}Pb$ ratios of between 1 and 3×10^{-4} (Arnould et al., 1997) and they are therefore, in principle, a suitable source of ^{205}Pb, as well as other s-process nuclides. However, it is widely considered that AGB stars are a more likely source because the respective stellar models are able to reproduce the abundances of most relevant short-lived nuclei relatively well. Spectroscopic observations have furthermore shown that AGB stars are enriched in s-process

elements, including Pb, but also Tc, which, given its short half-life ($t_{1/2} \approx 0.2$ Myr) has to be undergoing production in the star (Busso et al., 2003). The models for s-process nucleosynthesis in AGB stars are more complex but also relatively advanced. The most recent calculations for AGB stars inferred an initial $^{205}Pb/^{204}Pb$ of about 5×10^{-4} (Wasserburg et al., 1994; Busso et al., 2003) and this is again in excellent agreement with the value reported here. We emphasize that the consistency between astrophysical models and our measured value does not necessarily imply that s-process isotopes were injected late into the solar nebula. Due to the relatively long half-life of ^{205}Pb it is also possible that its abundance in the solar system merely reflects the steady-state galactic production rate and continuous injection into the ISM.

A particular problem of modeling the nucleosynthetic production of ^{205}Pb is the survivability of this nuclide in stars (Mowlavi et al., 1998). Hence, all estimates of its expected abundance are highly model dependent. At high temperatures ($>10^6$ K) the electron capture decay constant for ^{205}Pb is increased by several orders of magnitude, such that none should survive in stellar interiors. However, the daughter isotope ^{205}Tl undergoes a dramatic decrease in stability at $T > 10^8$ K and it β^- decays to ^{205}Pb even faster (Mowlavi et al., 1998). In general terms, the survival of ^{205}Pb is favored at higher stellar mass for a given metallicity and at lower metallicities for a given stellar mass. The results presented here, will therefore, provide new constraints on the minimum mass of the star responsible for the production of short-lived s-process nuclei, once detailed nucleosynthetic modeling is undertaken.

4.2. The initial $\varepsilon^{205}Tl$ of the solar system and implications for terrestrial accretion

The initial $\varepsilon^{205}Tl_{IAB,0} = -2.1 \pm 1.6$ calculated from the IAB metal isochron (Fig. 2a) is of particular interest because this can be used to estimate the initial Tl isotope composition of the solar system, $\varepsilon^{205}Tl_{SS,0}$. This is possible because there are several lines of evidence, which suggest that the IAB iron meteorites evolved from a parent body with a composition akin to chondrites (Benedix et al., 2000; Wasson and Kallemeyn, 2002). The high abundances of volatile elements determined for IAB irons furthermore imply a parent body more similar to carbonaceous or enstatite chondrites, as compared to volatile depleted ordinary chondrites (Benedix et al., 2000; Wasson and Kallemeyn, 2002). Based on this, it is assumed that the IAB parent body evolved with a $^{204}Pb/^{203}Tl$ of between 0 and 5, which encompasses the Pb/Tl ratios of carbonaceous, enstatite and the moderately volatile depleted H-chondrites (Wasson and Kallemeyn, 1988). In order to calculate the initial Tl isotope composition of the solar system, the inferred $\varepsilon^{205}Tl_{IAB,0}$ of -2.1 ± 1.6 was corrected for 15 ± 5 Myr of radiogenic ingrowth, with a $^{204}Pb/^{203}Tl = 2.5 \pm 2.5$. The calculation utilized a simple spreadsheet-based Monte-Carlo method, which combined the individual ($\pm 2\sigma$) uncertainties for a large randomly generated synthetic dataset and it yielded a result of $\varepsilon^{205}Tl_{SS,0} = -2.8 \pm 1.7$. This value is strikingly similar to the present day Tl isotopic composition of the bulk silicate Earth, which through analyses of various samples of the Earth's continental crust and mantle is constrained to be $\varepsilon^{205}Tl_{BSE} = -2.0 \pm 0.5$ (Nielsen et al., 2005, 2006).

The primary reason why the silicate portion of the Earth does not show a more radiogenic Tl isotope signature is that the material that accreted onto the Earth must have had a low Pb/Tl ratio, and this severely limited the ingrowth of radiogenic ^{205}Tl from the decay of ^{205}Pb. The results of modeling this effect are shown in Fig. 6. The model shown in this figure applies the same accretion scenario recently utilized by Halliday (2004), which features incremental growth, concomitant core formation, and an exponentially decreasing rate of growth. The step function that defines terrestrial accretion (see Fig. 1, Halliday, 2004) assumes runaway growth until the Earth has attained about 1% of its present mass. Further growth is simulated by successive additions of objects of 1% of the current mass of the Earth, until it reaches 10% of its present mass, then by 2% objects up to 30%, and then by 4% objects up to 90%. The Moon-forming Giant Impact, which contributes 9% of the total mass, occurs when the Earth attains about 90% of its current size, in accordance with the results of recent dynamic simulations (Canup and Asphaug, 2001).

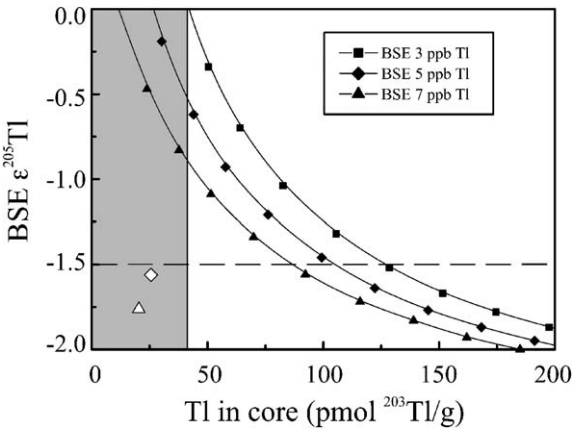

Fig. 6. Results, in terms of BSE Tl isotope compositions and core Tl concentrations, for terrestrial accretion models that yield reasonable Pb isotope systematics for the BSE. All models utilize $(^{205}Pb/^{204}Pb)_{SS,0} = 1.5 \times 10^{-4}$, $\varepsilon^{205}Tl_{SS,0} = -2.8$, and $\mu_{BE} = 0.7$. The three curves denote the results of standard accretion models (with no volatile loss) that yield reasonable BSE Tl concentrations of 3–7 ng/g. These standard accretion models achieve BSE $\varepsilon^{205}Tl$ values of less than -1.5 (dashed line) only if the Earth's core has high Tl contents. The shaded area displays the range of Tl concentrations determined for iron meteorites (including troilite inclusions). Also shown are the results of two models that incorporate late volatile loss (at the time of the Giant Impact), when 90% (open diamond; resulting in BSE = 5 ng/g Tl) and 85% (open triangle; resulting in BSE = 7 ng/g Tl) of the Pb and Tl present in the mantle are driven off. For these models, the accreting material is assumed to have a composition intermediate between CO and CV chondrites with $\mu = 0.42$ and 0.48 and $^{204}Pb/^{203}Tl = 2.6$ and 2.4, respectively. In both models the BE displays $\mu = 0.7$ after the Giant Impact.

After the giant impact, the model simulates a late veneer that contributes an additional 0.9% of the Earth's mass and a final 0.1% is delivered thereafter. The mean life of accretion, τ, which is the time required to achieve ~63% growth, was taken to be 15 Myr. This results in a Giant Impact that occurs at 43.5 Myr, which is similar to the most recent estimate of the age of the lunar magma ocean and thereby also the Moon (Kleine et al., 2005).

The isotopic models employed here assume that all impacting materials/planetesimals equilibrate fully with the silicate portion of the Earth prior to metal segregation and they furthermore apply ($^{205}Pb/^{204}Pb)_{SS,0} = 1.5 \times 10^{-4}$, $\varepsilon^{205}Tl_{SS,0} = -2.8$, $\mu_{BE} = 0.7$ ($\mu_{BE} \equiv$ bulk Earth $^{238}U/^{204}Pb$). The metal–silicate partition coefficients (D values) of Pb and Tl were then adjusted, such that models generated a BSE that is in accord with recent estimates, with regard to its Pb isotope composition, μ value (Halliday, 2004), Tl isotope composition $\varepsilon^{205}Tl_{BSE} = -2.0 \pm 0.5$; (Nielsen et al., 2005, 2006) and Tl concentration (3–7 ng/g; (Taylor and McLennan, 1985; McDonough and Sun, 1995)). This was achieved using metal–silicate D value of about 25 and 5–15 for Pb and Tl, respectively. In our standard models, no volatile loss occurs during accretion, and the Tl concentration of the accreting material and the metal–silicate partition coefficient of Tl were treated as free parameters.

The modeling results show that reasonable $\varepsilon^{205}Tl_{BSE}$ values of less than −1.5 can be achieved only if significant quantities of Tl partition into the core, yielding core concentrations for ^{203}Tl of greater than 80 pmol/g (Fig. 6). There are no published experimental constraints on the behavior of Tl during metal–silicate differentiation but it is noted that all iron meteorite samples (including troilites) analyzed in the present (Table 3) and previous studies (Chen and Wasserburg, 1987, 1994a) contain less than 40 pmol/g ^{203}Tl, and the majority display concentrations of $\ll$10 pmol/g ^{203}Tl. Of course, it is possible that the Earth's core has a much higher Tl content than iron meteorites due to changes in the partitioning behavior of Tl at high pressure; other elements such as Nb are thought to respond in such a fashion (Wade and Wood, 2001).

An alternative to consider is late-stage removal of Tl from the bulk silicate Earth. If it has not been added to the core, it must have been lost to space, possibly during the putative Moon-forming Giant Impact. Such models easily reproduce the composition of the BSE and also yield a Tl concentration in the core within the range observed for iron meteorites (Fig. 6). They do, however, require that more than about 80–90% of the Earth's Tl and Pb budget were driven off during the Giant Impact, which is assumed to have occurred at 43.5 Myr. Accretion with concomitant volatile loss also yields reasonable results, though because the Giant Impact provides significant amounts of Pb and Tl to the BE it is invariably necessary to simultaneously drive off a significant portion of Tl (and Pb) during the event in order to maintain Tl concentrations for BSE and the core that are in accord with the BSE estimates (Halliday, 2004) and iron meteorite results.

Strontium isotope data for lunar rocks are consistent with loss of 90% of the Rb from the material that formed the Moon between 10 Myr after the start of the solar system and the Giant Impact (Halliday et al., 2001). The loss of heavy elements from large planets is, however, dynamically difficult (Jones and Palme, 2000) but it is also supported by Xe isotopic evidence (Pepin and Porcelli, 2002) and it may be possible if volatile elements like Pb and Tl were atmophile (Halliday, 2004) in the hot magma ocean environment of the early Earth (Sasaki, 1990). In addition, it is notable that accretion models with late volatile element depletion are able to utilize low metal–silicate distribution coefficients for Pb ($D \approx 1$–10) that are in much better agreement with experimental results (Ohtani and Yurimoto, 1996) than those of the standard accretion models, which require $D \approx 25$.

5. Conclusions and outlook

In this study, we have determined the Tl isotope compositions and the Pb/Tl ratios of a number of iron meteorites, in search of evidence for the former existence of radioactive ^{205}Pb in the early solar system. Seven metal fragments from the IAB iron meteorites Toluca and Canyon Diablo define an isochron with a slope equivalent to $^{205}Pb/^{204}Pb = 7.4 \pm 1.0 \times 10^{-5}$ at the time of metal crystallization. Adoption of an I–Xe crystallization age for the IAB iron meteorites of 10–20 Ma after formation of the first solids, yields solar system initial values of $^{205}Pb/^{204}Pb_{SS,0} = 1.0$–$2.1 \times 10^{-4}$ and $\varepsilon^{205}Tl_{SS,0} = -2.8 \pm 1.7$.

It is difficult to reconcile these results with the present day Tl isotope composition of the bulk silicate Earth ($\varepsilon^{205}Tl = -2.0 \pm 0.5$) and the Pb–Tl budgets of iron meteorites, if the latter are assumed to constrain the composition of the Earth's core. Modeling of terrestrial accretion indicates that the Earth's Tl isotope systematics are most readily reconciled with the present data if either the bulk silicate Earth lost about 80–90% of its Tl and Pb budget during the accretion process, possibly in the putative Moon-forming Giant Impact, or if the Earth's core contains much larger amounts of Tl and Pb than what would be expected from iron meteorite studies.

Several lines of investigation can be pursued to further elucidate which of these two scenarios is more reasonable. The Tl isotope composition of CI carbonaceous chondrites should be determined because these meteorites are known to have formed early and they display very low Pb/Tl ratios, such that they should contain very little radiogenic Tl. As a consequence, Tl isotope data for CI chondrites can be used to provide significantly improved estimates of the initial Tl isotope composition of the solar system. It will furthermore be important to carry out metal–silicate partitioning experiments for Pb and Tl at high pressures. The results of these experiments are critical, because they will show whether the Earth's core can accommodate significantly larger Tl and Pb contents than those found in iron meteorites.

Acknowledgments

We thank T. McCoy (Smithsonian Institution) and R. Wieler (ETH) for providing samples, T. Kleine and H. Williams for fruitful discussions, and M. Meier, U. Menet, D. Niederer, B. Rütsche, C. Stirling, A. Süsli, S. Woodland, H. Williams, and the rest of the IGMR group at the ETH for keeping the mass spectrometers and clean labs functioning at all times. We are also grateful to M. Boyet, K. Rankenburg, and an anonymous referee for insightful reviews and R. Gallino, G. Wasserburg, and B. Wood for providing comments on earlier versions of this manuscript. This study was funded by research grants from the ETH Zurich, the Schweizerische Nationalfonds and the Danish Research Agency. This is publication number 425 in the ARC National Key Centre for Geochemical Evolution and Metallogeny of Continents (GEMOC).

Associate editor: Richard J. Walker

References

Anders, E., Stevens, C.M., 1960. Search for extinct lead 205 in meteorites. *J. Geophys. Res.* **65**, 3043–3047.

Arnould, M., Paulus, G., Meynet, G., 1997. Short-lived radionuclide production by non-exploding Wolf-Rayet stars. *Astron. Astrophys.* **321**, 452–464.

Benedix, G.K., McCoy, T.J., Keil, K., Love, S.G., 2000. A petrologic study of the IAB iron meteorites: constraints on the formation of the IAB-winonaite parent body. *Meteorit. Planet. Sci.* **35**, 1127–1141.

Bogard, D.D., Garrison, D.H., Takeda, H., 2005. Ar–Ar and I–Xe ages and the thermal history of IAB meteorites. *Meteorit. Planet. Sci.* **40**, 207–224.

Buchwald, V.F., 1975. *Handbook of Iron Meteorites*. University of California Press, Cambridge, p. 1418.

Burkland, M.K., Swindle, T.D., Baldwin, S.L., 1995. Isothermal heating experiments on Bjurbole—implications for the release mechanisms of radiogenic Xe-129. *Geochim. Cosmochim. Acta* **59**, 2085–2094.

Busso, M., Gallino, R., Wasserburg, G.J., 2003. Short-lived nuclei in the early solar system: a low mass stellar source? *Publ. Astron. Soc. Aust.* **20**, 356–370.

Canup, R.M., Asphaug, E., 2001. Origin of the Moon in a giant impact near the end of the Earth's formation. *Nature* **412**, 708–712.

Carlson, R.W., Hauri, E.H., 2001. Extending the Pd-107–Ag-107 chronometer to low Pd/Ag meteorites with multicollector plasma-ionization mass spectrometry. *Geochim. Cosmochim. Acta* **65**, 1839–1848.

Chen, J.H., Wasserburg, G.J., 1987. A search for evidence of extinct lead 205 in iron meteorites. *LPSC* **XVIII**, 165–166.

Chen, J.H., Wasserburg, G.J., 1990. The isotopic composition of Ag in meteorites and the presence of Pd-107 in protoplanets. *Geochim. Cosmochim. Acta* **54**, 1729–1743.

Chen, J.H., Wasserburg, G.J., 1994a. The abundance of thallium and premordial lead in selected meteorites—the search for ^{205}Pb. *LPSC* **XXV**, 245.

Chen, J. H., Wasserburg, G. J., 1994b. A search for ^{107}Ag and ^{205}Pb in meteorites. Abstracts of the Eighth International Conference of Geochr. Cosmochr. Isot. Geol. p. 55.

Chen, J. H., Wasserburg, G. J., 1996. Live ^{107}Pd in the early solar system and implications for planetary evolution. In: Basu, A., Hart, S.R. (Eds.), Earth Processes: Reading the Isotopic Code. AGU Monograph, pp. 1–20.

Choi, B.G., Ouyang, X.W., Wasson, J.T., 1995. Classification and origin of IAB and IIICD iron meteorites. *Geochim. Cosmochim. Acta* **59**, 593–612.

Göpel, C., Manhès, G., Allègre, C.J., 1985. U–Pb systematics in iron meteorites: uniformity of primordial lead. *Geochim. Cosmochim. Acta* **49**, 1681–1695.

Halliday, A.N., 2004. Mixing, volatile loss and compositional change during impact-driven accretion of the Earth. *Nature* **427**, 505–509.

Halliday, A.N., Lee, D.C., Porcelli, D., Wiechert, U., Schönbächler, M., Rehkämper, M., 2001. The rates of accretion, core formation and volatile loss in the early Solar System. *Philos. Trans. R. Soc. Lond. Ser. A—Math. Phys. Eng. Sci.* **359**, 2111–2134.

Herpfer, M.A., Larimer, J.W., Goldstein, J.I., 1994. A comparison of metallographic cooling rate methods used in meteorites. *Geochim. Cosmochim. Acta* **58**, 1353–1365.

Horan, M.F., Smoliar, M.I., Walker, R.J., 1998. ^{182}W and ^{187}Re–^{187}Os systematics of iron meteorites: chronology for melting, differentiation, and crystallization in asteroids. *Geochim. Cosmochim. Acta* **62**, 545–554.

Huey, J.M., Kohman, T.P., 1972. Search for extinct natural radioactivity of Pb-205 via thallium-isotope anomalies in chondrites and lunar soil. *Earth Planet. Sci. Lett.* **16**, 401–412.

Jones, J.H., Palme, H., 2000. In: Richter, K., Canup, R. (Eds.), *Origin of the Earth and Moon*. Univ. Arizona Press, pp. 197–216.

Jones, J.H., Hart, S.R., Benjamin, T.M., 1993. Experimental partitioning studies near the Fe–FeS eutectic, with an emphasis on elements important to iron meteorite chronologies (Pb, Ag, Pd, and Tl). *Geochim. Cosmochim. Acta* **57**, 453–460.

Kleine, T., Palme, H., Mezger, K., Halliday, A.N., 2005. Hf–W chronometry of lunar metals and the age and early differentiation of the Moon. *Science* **310**, 1671–1674.

Lee, D.-C., Halliday, A.N., 1996. Hf–W isotopic evidence for rapid accretion and differentiation in the early Solar system. *Science* **274**, 1876–1879.

Lodders, K., 2003. Solar system abundances and condensation temperatures of the elements. *Astrophys. J.* **591**, 1220–1247.

McDonough, W.F., Sun, S.-s., 1995. The composition of the Earth. *Chem. Geol.* **120**, 223–253.

Mowlavi, N., Goriely, S., Arnould, M., 1998. The survival of Pb-205 in intermediate-mass AGB stars. *Astron. Astrophys.* **330**, 206–214.

Nielsen, S.G., Rehkämper, M., Alt, J.C., Butterfield, D., Haase, K.M., Halliday, A.N., Ishibashi, J., Okamura, K., Sohrin, Y., 2004a. An elemental and isotopic study of the marine geochemistry of thallium. *Eos Trans. AGU* **84**, abstract OS42F-02.

Nielsen, S.G., Rehkämper, M., Baker, J., Halliday, A.N., 2004b. The precise and accurate determination of thallium isotope compositions and concentrations for water samples by MC-ICPMS. *Chem. Geol.* **204**, 109–124.

Nielsen, S.G., Rehkämper, M., Porcelli, D., Andersson, P.S., Halliday, A.N., Swarzenski, P.W., Latkoczy, C., Günther, D., 2005. The thallium isotope composition of the upper continental crust and rivers—an investigation of the continental sources of dissolved marine thallium. *Geochim. Cosmichim. Acta* **69**, 2007–2019.

Nielsen, S.G., Rehkämper, M., Norman, M.D., Halliday, A.N., Harrison, D., 2006. Thallium isotopic evidence for ferromanganese sediments in the mantle source of Hawaiian basalts. *Nature* **439**, 314–317.

Niemeyer, S., 1979. I–Xe dating of silicate and troilite from IAB iron meteorites. *Geochim. Cosmochim. Acta* **43**, 843–860.

Ohtani, E., Yurimoto, H., 1996. Element partitioning between metallic liquid, magnesiowustite, and silicate liquid at 20 GPa and 2500 °C: a secondary ion mass spectrometric study. *Geophys. Res. Lett.* **23**, 1993–1996.

Pengra, J.G., Genz, H., Fink, R.W., 1978. Orbital electron capture ratios in the decay of ^{205}Pb. *Nucl. Phys.* **A302**, 1–11.

Pepin, R.O., Porcelli, D., 2002. Origin of noble gases in the terrestrial planets*Noble Gases in Geochemistry and Cosmochemistry*, vol. 47. Mineralogical Society of America, Washington DC, pp. 191–246.

Pravdivtseva, O.V., Hohenberg, C.M., 2000. Iodine–xenon system in individual silicate grains from Toluca IAB. *Meteorit. Planet. Sci.* **35**, A131.

Quitte, G., Meier, M., Halliday, A.N., Latkoczy, C., Günther, D., 2005. Constraints on the formation of metal and sulphide in iron meteorites as inferred from nickel isotopes. *Eos Trans. AGU* **86**, abstract P41E-02.

Rehkämper, M., Halliday, A.N., 1999. The precise measurement of Tl isotopic compositions by MC- ICPMS: application to the analysis of geological materials and meteorites. *Geochim. Cosmochim. Acta* **63**, 935–944.

Rehkämper, M., Frank, M., Hein, J.R., Porcelli, D., Halliday, A., Ingri, J., Liebetrau, V., 2002. Thallium isotope variations in seawater and hydrogenetic, diagenetic, and hydrothermal ferromanganese deposits. *Earth Planet. Sci. Lett.* **197**, 65–81.

Rehkämper, M., Frank, M., Hein, J.R., Halliday, A., 2004. Cenozoic marine geochemistry of thallium deduced from isotopic studies of ferromanganese crusts and pelagic sediments. *Earth Planet. Sci. Lett.* **219**, 77–91.

Saikumar, V., Goldstein, J.I., 1988. An evaluation of the methods to determine the cooling rates of iron meteorites. *Geochim. Cosmochim. Acta* **52**, 715–726.

Sasaki, S., 1990. The primary solar-type atmosphere surrounding the accreting Earth; H_2O-induced high surface temperature. In: Newsom, H.E., Jones, J.H. (Eds.), *Origin of the Earth*. Oxford University Press, pp. 195–209.

Shen, J.J., Papanastassiou, D.A., Wasserburg, G.J., 1996. Precise Re–Os determinations and systematics of iron meteorites. *Geochim. Cosmochim. Acta* **60**, 2887–2900.

Taylor, S.R., McLennan, S.M., 1985. *The Continental Crust: Its Composition and Evolution*. Blackwell Scientific, p. 1–312.

Tsuchiyama, A., Kawamura, K., Nakao, T., Uyeda, C., 1994. Isotopic effects on diffusion in MgO melt simulated by the molecular-dynamics (Md) method and implications for isotopic mass fractionation in magmatic systems. *Geochim. Cosmochim. Acta* **58**, 3013–3021.

Wade, J., Wood, B.J., 2001. The Earth's 'missing' niobium may be in the core. *Nature* **409**, 75–78.

Wasserburg, G.J., Busso, M., Gallino, R., Raiteri, C.M., 1994. Asymptotic giant branch stars as a source of short-lived radioactive nuclei in the solar nebula. *Astrophys. J.* **424**, 412–428.

Wasson, J.T., Kallemeyn, G.W., 1988. Compositions of chondrites. *Phil. Trans. R. Soc. Lond. Ser. A* **325**, 535–544.

Wasson, J.T., Kallemeyn, G.W., 2002. The IAB iron-meteorite complex: a group, five subgroups, numerous grouplets, closely related, mainly formed by crystal segregation in rapidly cooling melts. *Geochim. Cosmochim. Acta* **66**, 2445–2473.

Weyer, S., Anbar, A.D., Brey, G.P., Munker, C., Mezger, K., Woodland, A.B., 2005. Iron isotope fractionation during planetary differentiation. *Earth Planet. Sci. Lett.* **240**, 251–264.

Williams, H.M., Halliday, A., Teutsch, N., Levasseur, S., 2004. Iron isotope fractionation in iron meteorites: new insights into metal–sulfide segregation and core crystallisation. *Eos Trans. AGU* **85**, F1251.

Wombacher, F., Rehkämper, M., Mezger, K., Munker, C., 2003. Stable isotope compositions of cadmium in geological materials and meteorites determined by multiple-collector ICPMS. *Geochim. Cosmochim. Acta* **67**, 4639–4654.

Woodland, S.J., Rehkämper, M., Halliday, A., Lee, D.-C., Hattendorf, B., Günther, D., 2005. Accurate measurement of silver isotope composition in geological materials including low Pd/Ag meteorites. *Geochim. Cosmochim. Acta* **69**, 2153–2163.